Investigating the emissions during acceleration of a turbocharged diesel engine operating with bio-diesel or n-butanol diesel fuel blends

Constantine D. Rakopoulos*, **Athanasios M. Dimaratos, Evangelos G. Giakoumis, Dimitrios C. Rakopoulos**

Internal Combustion Engines Laboratory, Department of Thermal Engineering,
School of Mechanical Engineering, National Technical University of Athens
9 Heroon Polytechniou St., Zografou Campus, 15780 Athens, Greece

ABSTRACT

Control of transient emissions from turbocharged diesel engines is an important objective for automotive manufacturers, since stringent criteria for exhaust emission levels must be met as dictated by the legislated transient cycles. On the other hand, bio-fuels are getting impetus today as renewable substitutes for conventional fuels (diesel fuel or gasoline), especially in the transport domain. In the present work, experimental tests are conducted on a turbocharged truck diesel engine in order to investigate the formation mechanism of nitric oxide (NO) and smoke under various accelerating schedules experienced during daily driving conditions. To this aim, a fully instrumented test bed was set up in order to capture the development of key engine and turbocharger variables during the transient events using ultra-fast response instrumentation for the instantaneous measurement of the exhaust NO and smoke opacity. Apart from the baseline diesel fuel, the engine was operated with a blend of diesel fuel with 30% bio-diesel, and a blend of diesel fuel with 25% n-butanol. Analytical diagrams are provided to explain the behavior of emissions development in conjunction with turbocharger and fueling response. Unsurprisingly, turbocharger lag was found to be the main culprit for the emissions spikes during all test cases examined. The differences in the measured exhaust emissions of the two bio-fuel/diesel fuel blends, both leading to serious smoke reductions but also NO increases compared with the baseline operation of the engine were determined and compared. The differing physical and chemical properties of bio-diesel and n-butanol against those of the diesel fuel, together with the formation mechanisms of NO and soot were used for the analysis and interpretation of the experimental findings concerning transient emissions.

---

* Corresponding author. Tel.: +30 210 7723529; fax: +30 210 7723531.
E-mail address: cdrakops@central.ntua.gr (C.D. Rakopoulos).

Nomenclature

C concentration (ppm)

k absorption coefficient (m^{-1} or cm^{-1})

L optical path length (m or cm)

m mass (kg)

MW molecular weight (kg/kmol)

N opacity (%)

p pressure (N/m^2)

R_m universal gas constant = 8314.3 J/kmol K

S dependent quantity

SD soot density (mg/m^3)

SMC soot mass fraction (mg/kg)

T temperature (K)

x_i independent variable

Abbreviations

EGR   exhaust gas recirculation

FSO   full scale output

HC   hydrocarbon

NO   nitric oxide

NO_2 nitrogen dioxide

NO_x nitrogen oxides

ppm   parts per million

rpm   revolutions per minute

TDC   top dead center

1.   Introduction

The turbocharged diesel engine is currently the preferred powertrain system in medium and medium-large unit applications (trucks, land traction, ship propulsion, electricity generation etc). Moreover, it is continuously increasing its share of the highly competitive automotive market, having already ensured a share comparable to that of the gasoline engine in Europe [1]. The most attractive feature of the diesel engine is its overall very good fuel efficiency, which can surpass a value of 40% in vehicular applications and even

50% in large, two-stroke units used for marine propulsion or electricity generation. Thus, diesel-engined vehicles achieve much lower fuel consumption and reduced carbon dioxide emissions than their similarly rated spark-ignition counterparts.

Traditionally, the study of diesel engine operation has focused on steady-state performance, with much less attention paid to transient operation. However, the majority of daily driving schedules involves transient conditions with only a very small portion of a vehicle's operating pattern being truly steady-state, e.g. when cruising on a motorway. Thus, the experimental and modeling investigation of diesel engine transient operation has turned out to be an important objective for engine manufacturers, intensified by the fact that significant deviations are experienced when comparing instantaneous transient emissions with their quasi-steady counterparts [2]. In particular, Hagena et al. [3] reported higher NO_x (nitrogen oxides) emissions by a factor of 1/3 and higher particulate emissions by an order of magnitude between instantaneous transient measurements and quasi-steady predictions. Rakopoulos and Giakoumis [4] reviewed, among other things, studies concerning emissions prediction during transient operation and their comparison with steady-state conditions. Additionally, Gullett at al. [5] studied organic air toxic pollutants emissions (e.g. benzene and naphthalene) during cold and hot starting and load changes and reported transient concentration values 15 times higher than their respective steady-state levels. Finally, Wijetunge et al. [6] focused on the behavior of operating parameters (e.g. boost pressure, EGR valve position) during transient operation and their effect on emissions development, reporting significant deviations between transient and steady-state hydrocarbon (HC) emissions.

Acknowledging the above mentioned findings, various legislative directives in the European Union [7], Japan [8] and the US [9] have drawn the attention of manufacturers and researchers to the transient operation of diesel engines in the form of transient cycles certification for new vehicles.

Although experimental studies of transient cycles are of particular importance [2], they provide 'mean' values of each emitted pollutant and so conceal the influence of each individual speed or load change in the cycle. Therefore, the importance of understanding and reducing transient emissions separately for each acceleration or load acceptance in the cycle becomes obvious. Only then can one study the contributing and controlling factors and so reach the correct measures needed for reduced overall emission values.

The fundamental aspect of transient conditions lies in their operating discrepancies compared with the respective steady-state ones (i.e. operation at the same engine speed

and fuel pump rack position). Whereas during steady-state operation, engine speed and fueling and so all the other engine and turbocharger properties remain essentially constant, under transient conditions both the engine speed and fuel supply change continuously. Consequently, the available exhaust gas energy varies, affecting turbine enthalpy drop and, through the turbocharger shaft torque balance, the boost pressure and air supply to the engine cylinders is influenced. However, due to various dynamic, thermal and fluid delays in the system (mainly originating in the turbocharger moment of inertia - turbocharger lag), combustion air supply is delayed compared to fueling, adversely affecting torque build-up and emissions [2].

However, the vital issue of emissions overshoot during transients [3] has not been investigated adequately, owing to the need for highly complicated, sophisticated and costly experimental equipment, such as fully-automated test beds with electronically controlled dynamometers and fast response exhaust gas analyzers. As a result, a relatively small amount of experimental work has been reported thus far. For example, Kang and Farell [10] studied HC and NO_x emissions during individual transient events in a high speed DI diesel engine. Black et al. [11] investigated NO_x emissions response during a legislated transient cycle, and further researched on appropriate transient control strategies. Additionally, Campbell et al. [12] performed transient gaseous and particulate emission measurements on a diesel passenger car equipped with an exhaust after-treatment device (diesel particulate filter). Finally, the present research group [13] recently published emission results during cold starting, acceleration and load change of a turbocharged diesel engine.

On the other hand, depleting crude oil reserves and growing prices have placed considerable attention in the development of alternative fuel sources, with particular emphasis on the bio-fuels that possess the added advantage of being renewable, showing an *ad hoc* advantage in reducing emitted carbon dioxide (CO_2) [14]. Bio-fuels made from agricultural products (oxygenated by nature) reduce the world's dependence on oil imports, support local agricultural industries and enhance farming incomes. Moreover, they offer benefits in terms of reduced smokiness or particulate matter from diesel engines. Among those, vegetable oils or their derived bio-diesels (methyl or ethyl esters) are considered as very promising fuels.

Experimental studies of emission measurements during steady-state and transient operation when using bio-diesel blends appear in various published works. Specifically, Starr [15] considered various fuels, including bio-diesel, in an experimental study of hot

start emissions of a heavy-duty diesel engine, while Graboski et al. [16] experimented on the same engine running on blends of No. 2 US diesel with bio-diesel and reported on its transient emissions. Sharp et al. [17] included three engines and three fuels in their investigation of transient emissions during legislated driving cycles, and Tsolakis et al. [18] researched on steady-state performance and emissions of a diesel engine fueled with diesel-rapeseed methyl ester (RME) blends focusing on EGR effects. Furthermore, Wang et al [19] used nine heavy trucks in order to study the effects of bio-diesel blends on emissions during a driving cycle, while Durbin et al. [20] tested off-road vehicles in various cycles (e.g. FTP, US06) fueled with a variety of alternative fuels. Karavalakis et al. [21] implemented a diesel engine powered passenger vehicle operated on the European and the Athens driving cycles using diesel-soy methyl ester blends in order to study gaseous and particulate emission profile. Luján et al. [22] considered the European light-duty driving cycle in their work for a common rail high speed diesel engine fueled with blends varying from 30% to 100% bio-diesel. Fontaras et al. [23] included various driving cycles in a study of regulated and non-regulated pollutant emissions of a Euro 2 passenger car running on bio-diesel fuel, while Tsolakis et al. [24] investigated the effects of exhaust gas fuel reforming on the emissions of diesel and homogeneous charge compressions ignition (HCCI) engines fueled with bio-fuels. Finally, Ferreira et al. [25] analyzed volatile organic compounds emissions from a diesel engine operating on bio-diesel blends under steady-state conditions.

All of the above mentioned works report decreases in smoke/particulate matter and moderate increases in NO emissions. Nonetheless, since most of the above (transient) investigations focus on transient cycle operation, they provide 'mean' values of each emitted pollutant and so conceal the influence of each individual speed or load change in the cycle, a gap that the current work aims to fill.

Apart from bio-diesel, a very challenging competitor for use as fuel in compression ignition engines is ethanol and, better still, butanol; surprisingly, both have not been extensively tested in diesel engines. Butanol is of particular interest as a renewable bio-fuel as it is less hydrophilic and it possesses higher heating value, higher cetane number, lower vapor pressure, and higher miscibility than ethanol; this makes it preferable to ethanol for blending with conventional diesel fuel.

The literature concerning the use of butanol/diesel fuel blends in diesel engines and its effects on their performance and exhaust emissions is very limited, a fact that constitutes another major aspect of the originality of the present work. Miers et al. [26], reported on a

drive cycle analysis of n-butanol/diesel blends in a light-duty turbo-diesel vehicle. Two more studies by Yoshimoto et al. [27,28] deal with the performance and exhaust emission characteristics of a diesel engine fueled with vegetable oils blended with oxygenated organic compounds, including ethanol and n-butanol. Also, Huang et al. [29] used a very small quantity of n-butanol only for the purpose of improving the solubility of the ethanol/diesel fuel blends used. The present research group recently presented the results of an experimental investigation on a Ricardo 'Hydra', high-speed, naturally aspirated, direct injection diesel engine of the automotive type [30]. These revealed the beneficial effects of using various blends of n-butanol with normal diesel fuel on the performance and exhaust emissions at various loads. Finally, Armas et al. have reported results of smoke opacity during various individual transients (as the ones considered in the present study) using either vegetable oil methyl esters [31] or bio-ethanol/diesel fuel blends [32].

The target of the present study is to investigate the effect of diesel blends with two challenging bio-fuels on the transient emissions of a turbocharged diesel engine during acceleration, and compare the results with the neat diesel operation case. The two blends considered here (no modifications were made on the engine side when using these bio-fuels) are blends of

- diesel with 30% by vol. bio-diesel and
- diesel with 25% by vol. n-butanol (normal butanol).

The experimental tests were conducted on a medium-duty, turbocharged and after-cooled, direct injection diesel engine, with the use of fast response emission measurement instrumentation. The experimental investigation focused on the measurement of the two most influential diesel engine pollutants, i.e. nitric oxide (NO) and smoke (in terms of opacity). Since the engine is intended for automotive applications, the testing schedule was limited to individual acceleration events. By so doing it was possible to derive instantaneous (in contrast to the usually applied 'mean value') transient emission results, which can better help understanding of the complex underlying phenomena.

The instantaneous emission results are discussed in conjunction with the fuel blends composition and properties, as well as with the engine and turbocharger transient response. The differing physical and chemical properties of bio-diesel and n-butanol among themselves and against those of the diesel fuel are used for the analysis and interpretation of the experimental findings. It is, thus, believed that light is shed into the

combustion as well as the formation mechanisms of NO and soot during transient conditions.

2. Experimental test bed installation

A general layout of the test bed installation, the instrumentation used and the data acquisition system is illustrated in Fig. 1. A brief description of the individual components is given in the following subsections.

2.1 Engine under study

The engine used in this study is a Mercedes-Benz OM 366 LA, turbocharged and after-cooled, direct injection diesel engine, following the Euro II emissions standard. It is widely used to power mini-buses and small/medium trucks. Its basic technical data are given in Table 1. Two notable features of the engine are, on the one hand its retarded fuel injection timing in order to achieve low NO emissions and, on the other hand, the fuel-limiter (cut-off) function. The latter is practically an aneroid device controlling the fuel pump rack maximum travel according to boost pressure in order to limit the exhaust smoke level during demanding conditions such as, heavy transients or low-speed, high-load steady-state operation. The engine is coupled to a hydraulic dynamometer, which allows a good simulation of a vehicle's acceleration as will be explained later.

2.2 Emissions measurement

2.2.1 Nitric Oxide (NO) measurement

For the continuous measurement of NO emissions, the ultra-fast response analyzer CLD500 by Cambustion Ltd. [33] is employed. This is a chemiluminescent detector used for measuring NO and NO_x (in the latter case incorporating a NO_2 to NO converter) concentration in the exhaust gas with a 90%-10% response time of approximately 2 ms for NO and 10 ms for NO_x [34]. These very short response times are achieved by locating the detectors in remote sample heads, which are positioned very close to the sample point in the engine, and by conveying the sample gas to the detectors under the influence of a vacuum through narrow heated capillaries. The linearity of the analyzer is less than ±1% FSO (full scale output), its drift is less than ±1% FSO per hour and its accuracy is 5 ppm.

The CLD500 equipment has two remote sampling heads controlled by a mains control unit and it is capable of simultaneous sampling at two different locations. For the current

study, the two sampling (head) positions are shown in Fig. 1. The first head is located exactly after the exhaust valve of cylinder No. 1 (this is the same cylinder from which the indicator diagrams were taken) capturing the individual cylinder's NO concentration, and the second head is located downstream of the turbocharger capturing total NO emission concentration. In this study, only the second sampling head was applied.

It should be mentioned at this point that we selected to measure only NO concentration, owing to the very low values of NO_2/NO_x ratio generally experienced in diesel engines, particularly at the conditions experienced during abrupt transients. To this aim, the CLD500 analyzer used was not equipped with the NO_2 to NO converter.

2.2.2 Opacity measurement

The exhaust gas (smoke) opacity is measured continuously with the AVL 439 partial flow Opacimeter. This is a device particularly suitable for dynamic testing measurements with the exhaust gas sample flowing continuously through the opacimeter with a constant flow rate. The response time of the opacimeter is less than 0.1 s and its accuracy is 0.1% opacity. The opacity of the sample is determined from the measurement of the attenuation of visible light by the smoke in the exhaust gas sample located between the light source and the detector unit [35]. The opacimeter outputs the measurement either in terms of opacity values N (0–100%), as in the case of the present study, or absorption coefficient values k (0–10 m^{-1}). Its technical characteristics comply with legal requirements such as ECE R24, SAE J 1667 and the ELR test cycle, with the respective filter algorithms pre-programmed into the opacimeter. In this study, no filter algorithm was applied ('raw' signal) in order to capture successfully with no loss of information all the smoke emission peaks. The location of sampling and return lines, as can be seen in Fig. 1, is downstream of the turbocharger.

2.3 Measurement of engine and turbocharger operating parameters

The engine and turbocharger operating parameters measured and recorded continuously are: engine speed; cylinder pressure; fuel pump rack position; boost pressure and turbocharger speed. The location of each measuring device on the experimental test bed installation is shown in Fig. 1. Table 2 provides a brief list of the various measuring devices together with their measuring error; a more detailed description can be found in Ref. [13]. A custom made 'stop' with various adjustable positions, each one corresponding to a specific engine speed, was fitted on the (accelerator) pedal in

order to ensure constant pedal position at the end of each acceleration test as well as repeatability of the accelerations.

Inlet and exhaust pressures and temperatures at various locations were also measured during steady-state conditions with conventional analogue devices. Additionally, fuel consumption measurements were undertaken during steady-state operation with the use of a gravimetric fuel tank.

2.4 Data acquisition and processing system

All the above mentioned signals from the measuring devices and instruments are fed to the input of the data acquisition module, which is a Keithley KUSB 3102 ADC card connected to a Pentium Dual Core PC via USB interface. The specific card has a maximum sampling rate of 100 ksamples/s, with a 12-bit resolution for its 8 differential analogue inputs. Following the storage of the recorded measurements into files, the data were processed using an in-house developed computer code.

3. Properties of fuels tested and their blending

The conventional diesel fuel used was supplied by the Aspropyrgos Refineries of the 'Hellenic Petroleum SA' and represents the typical, Greek automotive, low sulfur (0.035% by weight) diesel fuel; it formed the baseline fuel of the present study.

The bio-diesel used was a mixture of 50% - 50% methyl esters (ME) originating from sunflower and cottonseed oils, respectively. Blend of 30% (by vol.) of this was prepared by mixing with the conventional diesel fuel.

The methyl esters were supplied from and produced at the Chemical Process Laboratory of the School of Chemical Engineering, of the National Technical University of Athens (NTUA), via transesterification with methanol of the corresponding feedstock raw material at a Pilot Plant using KOH as catalyst; they were tested according to the EN 14214 standards [36]. The original vegetable oils (sunflower and cottonseed) were produced from Greek feedstock and obtained from Greek commercial processing facilities.

The isomer of butanol (C_4H_9OH) n-butanol (otherwise called 1-butanol), having a straight-chain structure and the hydroxyl group (-OH) at the terminal carbon, was used in the present study. It was of 99.9% purity (analytical grade). A blend of 25% (by vol.) of this was prepared by mixing with conventional diesel fuel. Preliminary evaluation tests on the solubility of n-butanol in the diesel fuel with blending ratios up to 50%/50% proved,

actually, that the mixing was excellent with no phase separation for a period of several days. Thus, no emulsifying agent was necessary as would be the case with ethanol [37].

It was decided to use a rather high blending ratio of both alternative fuels with conventional diesel oil in order for the differences to be more prominent and the underlying mechanisms better understood.

Table 3 summarizes the properties of the diesel fuel, the two methyl esters (their properties are similar) constituting the bio-diesel, and n-butanol. With the exception of the density and lower calorific values that were used in the computations, all the other cited properties are referred here for comparative purposes, in order to explain qualitatively the relative emissions behavior of the different fuel blends.

4. Post-processing of the experimental data

4.1 Calculation of nitric oxide (NO) mass per engine cycle

The measured concentration values of NO (in ppm) during transient testing are converted into mass values (mg/cycle) using the following relationship

$$m_{NO} = \frac{C_{NO}}{1000} \cdot \frac{MW_{NO}}{MW_{eg}} \cdot m_{eg} \qquad (1)$$

where C_{NO} is the measured NO concentration (in ppm), MW_{NO} and MW_{eg} are the NO and exhaust gas molecular weights, respectively, and m_{eg} is the exhaust gas mass per engine cycle. The latter includes both air and fuel mass. The in-cylinder trapped air mass is calculated by applying the perfect gas equation of state at the inlet valve closing event (IVC), using the measured values of boost pressure and temperature. For the calculation of total air mass, an estimation of the trapping efficiency (0.85-0.90) is needed. On the other hand, the fuel mass supply during each cycle of the transient event is found using the steady-state fuel pump operating curves for the instantaneous measured fuel pump rack position. The latter measurement provides the volumetric fuel supply which is converted to mass supply using each fuel blend's density.

4.2 Calculation of soot mass per engine cycle

In order to calculate the total soot mass emitted during the tests, the following procedure is applied [38]. Initially, the absorption coefficient is calculated from the opacity value

$$k = \frac{-\ln\left[1 - \dfrac{N}{100}\right]}{L} \qquad (2)$$

and so the soot density (*SD*) is derived by (in mg/m³)

$$SD = \frac{10^6 \cdot 1000 \cdot k}{S_p} \qquad (3)$$

where S_p is a constant depending on the temperature of the sample inside the opacimeter [38].

Soot density is expressed in mg soot per m³ of exhaust gas and can be further converted in mg soot per kg of exhaust gas (soot mass concentration – *SMC*) by dividing it with the exhaust gas density inside the measuring chamber of the opacimeter

$$SMC = \frac{SD}{\rho_{eg}} = \frac{SD}{\left[\dfrac{p_{eg} \cdot MW_{eg}}{R_m \cdot T}\right]} \qquad (4)$$

where p_{eg} is the sample pressure in the opacimeter (usually equal to atmospheric pressure). Finally, soot mass (in mg) can be found by multiplying *SMC* with the exhaust gas mass

$$m_{soot} = SMC \cdot m_{eg} \qquad (5)$$

For the case of the AVL Opacimeter 439 used in this study, the optical path length *L* is 43 cm and the sample temperature *T* is 373 K.

4.3 Error analysis

For the present work, the experimental error analysis consists of two components:
  i)   identifying the measuring error (accuracy) of each device implemented in the test bed installation,
  ii) calculating the uncertainty of the computed values of the various parameters resulting from the post processing of the measured data.

Concerning the first part, the third column of Table 2 provides the accuracy of the measurements of the engine and turbocharger operating parameters, as declared by each device manufacturer. As far as the accuracy of emission measurements is concerned, this has been given in subsections 2.2.1 and 2.2.2 for NO and opacity measurements respectively.

On the other hand, the uncertainty of the computed values of the various parameters is calculated following the methodology described in Ref. [39], which is based on the route

mean square method. For the general case, the uncertainty ΔS in the estimated value of a quantity S, depending on the independent variables x_1, x_2 … x_n (i.e. $S=S(x_1, x_2 … x_n)$) having individual errors Δx_1, Δx_2 … Δx_n respectively, is given by

$$\Delta S = \sqrt{\left(\frac{\partial S}{\partial x_1}\Delta x_1\right)^2 + \left(\frac{\partial S}{\partial x_2}\Delta x_2\right)^2 + … + \left(\frac{\partial S}{\partial x_n}\Delta x_n\right)^2} \qquad (6)$$

For the current study, the independent variables are the measured values of the various operating parameters (engine speed, boost pressure etc.) and the exhaust emissions. The estimated quantities are the NO and soot mass per engine cycle and their uncertainty is calculated by applying the above methodology for Eqs. 1 and 2–5 respectively. The resulting uncertainty is of the order of 2.5% for both pollutants (NO and soot mass). The latter value is considered acceptable for the comparison purposes between the various fuel blends investigated.

5.   Experimental procedure

The experimental matrix included various cases of acceleration, given that the engine is indented for automotive applications. Since the engine is coupled to a hydraulic dynamometer, during all acceleration cases the brake load (resistance) increased accordingly. This is actually the case when a vehicle accelerates in real-world driving; the increase in engine/vehicle speed results in an increase of both tire rolling and aerodynamic resistance. In all test cases, the engine was allowed to stabilize at the initial steady-state condition and then the pedal was pushed to the end of the adjustable custom made 'stop' to accelerate the engine.

The acceleration tests were performed for various combinations of initial engine rotational speed and load, mimicking vehicle real acceleration under various (vehicle) speeds and gears; the details are given in Table 4. Also, Fig. 2 provides an illustration of the initial and final conditions of each test in a speed-load graph.

Initially, all tests were conducted with the engine running on neat diesel fuel, constituting the 'baseline' to which the corresponding cases are compared when using the blends of diesel with bio-diesel or n-butanol. The same tests were performed for each fuel blend (described previously) assuring the best possible repeatability, through the custom made 'stop' fitted on the accelerator pedal. For every fuel change, the fuel lines were cleaned and the engine was left to run for a sufficient period of time to stabilize at its new condition. Additionally, a preconditioning procedure was followed between each fuel change in order to remove the deposited particulate matter on the exhaust pipe walls,

which could be blown out and released during the following tests [40] and, thus, leading to faulty measurements of smoke opacity and erroneous interpretations for each fuel blend and its effects on smoke emission.

6.   Experimental results and discussion

The discussion of the results and their interpretation in this section focuses primarily on the fuel property effects on the engine operating characteristics (injection, fuel spray development and combustion processes), and performance and emissions developed during acceleration. The analysis of the phenomena experienced during transient engine operation (e.g. turbocharger lag), affecting decisively performance and emissions, has been detailed recently in a previous publication by the present research group [13] (for the engine in hand), and will only be outlined here for the sake of brevity of this paper's space.

As it has long been established, turbocharger lag is the most notable off-design feature of diesel engine transient operation that significantly differentiates the torque pattern from the respective steady-state conditions. It occurs because, although the fuel pump responds rapidly to the increased fueling demand after a speed (or load) increase, the turbocharger compressor air-supply cannot match this higher fuel-flow instantly, but only after a number of engine cycles owing to the mechanical, flow and thermal inertia of the whole system, as there is no mechanical connection between engine crankshaft and turbocharger shaft. The above phenomenon is enhanced by the unfavorable turbocharger compressor characteristics at low engine speeds and loads (boost pressure depending strongly on turbocharger rotational speed). As a result of this slow reaction, the relative air-fuel ratio during the early cycles of the acceleration assumes very low values (even lower than stoichiometric), thus deteriorating combustion and leading to slow engine torque and speed response and long recovery period [2].

An example of this behavior is provided in Fig. 3. The lower sub-diagram shows the fuel pump rack response and boost pressure development during a typical acceleration event, with the engine running on neat diesel fuel. However, the qualitative remarks concerning engine and turbocharger response hold also true for the other fuels examined here. Fuel pump rack reaches its maximum position in four engine cycles, while at the same time interval (the well known turbocharger lag period) boost pressure remains practically unchanged, needing almost thirty cycles to reach its maximum value.

This mismatch between fueling and air-supply has a direct impact on pollutant emissions development, as revealed in the upper sub-diagram of Fig. 3. Both nitric oxide

(NO) concentration and smoke opacity assume peak values during the turbocharger lag period, which are much higher compared with their final steady-state ones (for the case of opacity this is an order of magnitude higher). Rapid increases in fuel injection pressure upon the onset of a (instantaneous) transient event cause the penetration of liquid fuel jet to increase. The higher-momentum fuel jet is not accompanied by equally enhanced gas motion, resulting in increased liquid fuel impingement on the cool combustion chamber walls, lower mixture preparation rate and greater heterogeneity of the mixture [13]. Additionally, the subsequent harder combustion course prolongs combustion and reduces the available time for soot oxidation. On the other hand, local high temperatures due to close to stoichiometric air-fuel mixtures, formed because of the still low air-supply, are expected to increase NO formation during the turbocharger lag cycles.

The above qualitative analysis concerns the most notable off-design feature of diesel engine transient operation, i.e. turbocharger lag. It applies in all cases detailed in the following subsections and, thus, will not be discussed again there. It is noted, however, that each individual test's characteristics differentiate the quantitative results concerning engine and turbocharger response, as well as emissions development during the transient event. This is why the previous example was given for a typical case of engine acceleration without any quantitative remarks.

The basic Figs. 4, 8 and 11 to be discussed in the following subsections with reference to Tests No. 1, 2 and 3 (Table 4), respectively, are eight-folded, comprising the response (with respect to time or equivalently cycle number) of six engine and turbocharger operating parameters (lower 6 sub-diagrams) as well as the development of the two exhaust pollutant emissions, i.e. nitric oxide (NO) in ppm and smoke opacity (%).

Specifically, the oxygen mass percentage parameter shown is found by computation from the in-cylinder trapped air mass, calculated as explained in subsection 4.1 above, and the fuel pump rack position in conjunction with the pump characteristics (functions of speed and load). This oxygen mass includes both the one in the air and the bound one in the fuel, and it is normalized with respect to the in-cylinder trapped air mass; this is why a level value of 23.3% (the oxygen content by weight of pure air) is shown when 'neat' diesel fuel is used in the tests. Of course, the extra oxygen in the fuel is very small with respect to its value in air, but it is important for the combustion phenomena and so emissions formation as it actually exists in crucial places and time instants mainly where a deficiency of oxygen exists; this is characteristic of the diesel engine nature of heterogeneous mixture formation and combustion.

6.1 Test No. 1

Fig. 4 presents the results for the first acceleration test (Test No. 1 in Table 4), for the response of the six engine and turbocharger operating parameters and the two pollutant emissions, as explained above. The specific test is particularly demanding both for the engine and the turbocharger, since the latter accelerates from almost zero boost.

For all three blends, fuel pump rack responds almost instantly to the fueling increase command and shifts to its maximum position in three engine cycles. Then, it gradually moves backwards to reach its final steady-state position, which is practically the same for all fuel blends. The (almost) identical fuel pump rack movement provokes the same acceleration rates for the three fuels, with very minimal differentiations observed only for the diesel/n-butanol blend. The same findings hold true for the turbocharger speed and boost pressure developments. It must be noted here that such slight deviations are unavoidable in a non-electronically controlled test bed. However, the deviations observed here are very modest and are not expected to affect the results and especially the general trends of each fuel blend examined.

As far as pollutant emissions are concerned, significant differences are observed for the three fuels studied. Particularly, smoke opacity presents great deviations, as is made clearer in Fig. 5 that gives an expanded view of opacity development during the acceleration Test No. 1. Both fuel blends improve (decrease) smoke emissions of the engine during this demanding transient event, with a follow on improvement observed at the final steady-state condition. Also, the improvement in smoke emission reduction is better for the n-butanol blend than the bio-diesel blend case. This also holds true for their cumulative values and in the same order as will be discussed later with respect to Fig. 7.

Although fuel injection and spray development differ slightly from the case of neat diesel fuel [41], we feel this behavior is due to the engine running effectively overall 'leaner' with respect to the neat diesel fuel case, since the trapped relative air-fuel ratio remains essentially the same, with the combustion being now assisted by the presence of the fuel-bound oxygen of the bio-diesel or n-butanol in locally crucial rich zones, which seems to have the dominant influence [30]. This is further supported by the oxygen mass percentage curves of the relevant subfigure of Fig. 4, as already discussed in Section 6 above. Moreover, the same subfigure reveals the always higher oxygen mass percentage of the n-butanol blend relative to the bio-diesel one that results to its superior behavior.

14

The peak opacity value is lowered by about 40% for the bio-diesel blend, while for the n-butanol blend the decrease reaches almost 73% compared with the neat diesel fuel. The exact percentage changes for the two fuel blends examined, compared with the baseline 100% diesel fuel, are given in Table 5.

On the other hand, NO emissions increase for the two specific fuel blends. These differences continue at the final steady-state condition. Moreover, the NO increase is higher for the bio-diesel blend than the n-butanol blend case. This also holds true for their cumulative values and in the same order as it will be discussed later with reference to Fig. 7. Again, although fuel injection and spray development differentiate slightly from the ones of the neat diesel fuel case [41], it is felt that this behavior is predominantly attributed to the strong dependence of NO formation on cylinder gas temperature that is confirmed for all three fuels in Fig. 6. Nitric oxide concentration follows closely the development of the maximum values of the global cylinder gas temperature, which is the one main parameter apart from the local oxygen availability affecting the very complex NO formation mechanism. This temperature has been calculated by applying the ideal gas state equation at the crank angle where the maximum cylinder pressure appears.

It is likely that lower temperatures may exist for the bio-diesel and the n-butanol cases as the engine runs overall 'leaner'. In the case of bio-diesel this lower temperature may also be attributed to its lower calorific value. By the same token, in the case of n-butanol this lower temperature may be attributed also to its lower calorific value and higher heat of evaporation, although these can somehow be offset by the opposing effect of the lower cetane number (and thus longer ignition delay) of the n-butanol leading possibly to higher temperatures during the premixed part of combustion when NO is predominantly formed. The higher values, however, with respect to the neat diesel fuel case suggest that the other main influential parameter, i.e. the local oxygen availability, has the dominant effect. With reference to the relevant subfigure of the oxygen mass percentage of Fig. 4, as discussed in Section 6 above, the higher values of the fuel-bound oxygen for the bio-diesel blend and the n-butanol one against the neat diesel fuel case may be bringing locally the 'prepared' mixture nearer to stoichiometry (towards the lean) during the premixed phase (when NO is mainly formed), thus leading to the relative increase of NO formation. Then, the higher values of NO for the bio-diesel blend compared with the n-butanol blend case could be explained by the fact that the higher values of the fuel-bound oxygen for the n-butanol blend against the bio-diesel blend case may render locally over-

lean the 'prepared' mixture during the premixed phase, thus leading to its relative mitigation of formation.

In any case, the leanness and the temperature of the mixture on a local basis form a delicate balance on NO formation weighting more or less on the one or the other side, depending on the type of blends and the specific engine calibration and its operating conditions.

For the acceleration case studied here, the percentage change in NO peak values is 31.7% and 28.7% for the bio-diesel and n-butanol blends, respectively, compared to the neat diesel fuel case (see Table 5).

The impact of the differences in the instantaneous pollutant emissions during this acceleration test on the cumulative NO and soot emissions values is made apparent in Fig. 7. The instantaneous NO concentration and smoke opacity values have been converted into mass values following the procedure described in Section 4 above, and the summation was executed until each case equilibrates. The same observations as for the instantaneous values apply also for the cumulative ones. Total NO mass exhausted during this transient event is increased by 23.8% for the bio-diesel blend and 12.9% for the n-butanol blend, while the decrease in cumulative soot mass for the two blends is 25.7% and 57.9%, respectively, compared to the nominal case (neat diesel fuel). It is noted here that the percentage differences of cumulative NO and soot mass are much higher than the uncertainty of their calculation (subsection 4.3). This proves that these differences are clearly attributed to the effect of the fuel blends used in this study on pollutants formation, and not on measuring or computation errors. This applies also to the other tests conducted in the present investigation.

6.2 Test No. 2

Fig. 8 shows the results for the transient Test No. 2 (Table 4). Here, acceleration from an initial speed of 1530 rpm to a final speed of 2080 rpm is performed. The brake loading increased accordingly (from 10% to 20%), since the brake connected to the engine is a hydraulic one; its torque rises with the second power of speed – the same applies also for the aerodynamic resistance term for vehicular applications. However, both initial and final load values remained overall low. As with the previous test, the response for the six engine and turbocharger operating parameters and the two pollutant emissions is given in this figure.

16

As with Test No. 1, the fuel pump rack movement is practically the same for all three fuel blends in Test No. 2 where it instantly shifts to its maximum position, reaching gradually its final steady-state one. Thus, engine speed follows the same profile in all cases, with the turbocharger speed and boost pressure developments following accordingly.

It is the pollutant emissions values again that show great differences for the bio-diesel and n-butanol blends compared with the baseline case of neat diesel fuel. The same qualitative trends are noticed as in Test No. 1 (Fig. 4). Nitric oxide emissions are increased for both blends, with the peak value being higher by about 44% for the bio-diesel blend and by almost 34% for the n-butanol one, as shown in Table 5, compared with the neat diesel fuel baseline case. The well known dependence of NO formation on cylinder gas temperature is again confirmed through the similarity between the NO concentration development and the maximum cylinder pressure profile; the former follows closely every local peak of the latter. The same trends apply also for the final steady-state values of each blend.

As far as smoke emissions are concerned, smoke opacity assumes significantly lower values for both fuel blends. An expanded view of opacity development during this test, Fig. 9, reveals a significant reduction of its maximum values, which is of the order of 13% for the bio-diesel blend and around 50% for the n-butanol one (summarized in Table 5), compared with the nominal case of neat diesel fuel.

The same observations as for the instantaneous values hold also true for the cumulative ones, as these are presented in Fig. 10. Total NO mass exhausted during acceleration Test No. 2 is increased by 50.6% for the bio-diesel blend and 36.2% for the n-butanol blend, while the decrease in cumulative soot mass for the two blends is 21.8% and 38.9%, respectively, compared with the nominal case (neat diesel fuel).

The theoretical explanations for the observed relative behavior of the two blends and the neat diesel fuel cases, with respect to the emitted NO and smoke emissions, are qualitatively the same as discussed in detail in the previous subsection 6.1, and are not repeated here.

6.3 Test No. 3

The last test conducted in this study (Test No. 3) is practically the same with the immediately previous one (Test No. 2) in terms of engine acceleration (same initial and final speed limits), differing only in the initial engine loading. Such tests represent the

different gear engaged in the gearbox when vehicular applications are concerned. Here, a medium initial load was chosen, with the final load affected accordingly, as detailed in Table 4 and Fig. 2. As with the previous tests, Fig. 11 presents the response for the six engine and turbocharger operating parameters and the two pollutant emissions during this acceleration case.

In all three cases, the fuel pump rack responds in the same manner (Fig. 11), shifting initially to a first peak position and then followed by a smoother movement to the maximum position. The latter behavior highlights in the most explicit way the fuel limiter operating principle that does not allow sharp fueling increases when the boost pressure is still low. As can be seen in Fig. 11, a small difference occurred in fuel pump rack movement for the case of the n-butanol blend, affecting accordingly engine speed response as well as turbocharger speed and boost pressure development. Unfortunately, as mentioned earlier, such moderate deviations are unavoidable in a non-electronically controlled test bed. However, the difference in terms of engine speed is slight and, thus, not affecting the qualitative remarks and general trends concerning each fuel blend studied.

As far as pollutant emissions are concerned, the same trends as for the previous two tests apply also here. Both the bio-diesel and the n-butanol blends increase NO emission and decrease smoke opacity. The interesting finding, however, here is that although maximum cylinder pressures, thus temperatures, are similar for the three blends, NO concentration values differ in a much greater extent than in the previous tests, during both transient and steady-state operation, highlighting and confirming in this way the very complex process of NO formation exposed earlier. Peak NO concentration values increase by about 52% for the bio-diesel blend and by around 35% for the n-butanol blend, while smoke opacity decreases by almost 30% and about 56% for the two blends, respectively, as depicted in Table 5.

Finally, as illustrated in Fig. 12, cumulative NO mass values are 25.2% and 21.9% higher, while the reduction in the total soot mass reaches 38.5% and 56.6% for the bio-diesel and the n-butanol blends, respectively, compared with the baseline case (neat diesel fuel).

Again, the theoretical explanations for the observed relative behavior of the two blends and the neat diesel fuel cases, with respect to the emitted NO and smoke emissions, are qualitatively the same as discussed in detail in the previous subsection 6.1, and are not repeated here.

7. Summary and conclusions

A fully instrumented test bed installation has been developed, in order to study the transient performance and emissions of a turbocharged and after-cooled diesel engine when fueled with bio-fuel/diesel blends. Fast response exhaust gas analyzers were employed for measuring nitric oxide and smoke emissions. The tested fuel blends were 100% ('neat') diesel fuel, 70%-30% diesel/bio-diesel, and 75%-25% diesel/n-butanol. A variety of acceleration events experienced during daily driving conditions was performed, as the engine is intended for automotive applications.

The basic conclusions derived from the current investigation, for the specific engine-hydraulic brake configuration and the fuel blends in hand, are summarized below:

- As expected, turbocharger lag was found to be the most notable contributor for all transient discrepancies experienced, independently from the fuel blend used, and the major cause for the overshoot of NO and smoke during transients.

- Peak or cumulative values of nitric oxide emission increased in all cases for the two fuel blends compared with the neat diesel fuel case, with the leanness and the temperature of the mixture on a local basis playing the decisive roles.

- A clear trend was distinguished according to which the increase in NO emission (peak or cumulative values) was greater for the bio-diesel blend compared with the n-butanol blend, with the leanness and the temperature of the mixture on a local basis playing the leading roles as above.

- For the test cases examined here, NO concentration peak value increased up to about 52% and 35% respectively for the biodiesel and n-butanol blends. The respective increase in cumulative values reached 50.6% and 36.2%, compared with the neat diesel fuel case.

- Peak or cumulative values of smoke opacity decreased in all cases for the two fuel blends compared with the neat diesel fuel case, with the relative fuel-bound oxygen mass playing the dominant role.

- A clear trend was distinguished according to which the reduction in smoke opacity values (peak or cumulative values) was higher for the n-butanol blend compared with the bio-diesel blend, with the relative values of fuel-bound oxygen mass playing again the dominant role.

- For the test cases examined here, peak values of smoke opacity decreased up to about 40% and 73% respectively for the biodiesel and n-butanol blends. The

respective decrease in cumulative values reached 38.5% and 57.9%, compared with the neat diesel fuel case.

Acknowledgements

References

[1] European Automobile Manufacturers' Association (ACEA). See also: <www.acea.be> [accessed 12/02/2010].

[2] Rakopoulos CD, Giakoumis EG. Diesel engine transient operation. London: Springer; 2009.

[3] Hagena JR, Filipi ZS, Assanis DN. Transient diesel emissions: analysis of engine operation during a tip-in. SAE paper no. 2006-01-1151, 2006.

[4] Rakopoulos CD, Giakoumis EG. Review of thermodynamic diesel engine simulation under transient operating conditions. SAE paper no. 2006-01-0884, 2006.

[5] Gullett BK, Touati A, Oudejans L, Ryan SP. Real-time emissions characterization of organic air toxic pollutants during steady-state and transient operation of a medium duty diesel engine. Atmos Environ 2006;40:4037-47.

[6] Wijetunge RS, Brace CJ, Hawley JG, Vaughan ND, Horrocks RW, Bird GL. Dynamic behaviour of a high speed direct injection diesel engine. SAE paper no. 1999-01-0829, 1999.

[7] European Commission, Enterprise and Industry – Automotive Section: Directives and regulations on motor vehicles; 2009. See also: <ec.europa.eu/enterprise/sectors/automotive/documents/directives/motor-vehicles/> [accessed 15/02/2010].

[8] DieselNet, Ecopoint Inc., Emission Test Cycles, European Transient Cycle (ETC); 2000. See also: <www.dieselnet.com/standards/cycles/etc.html> [accessed 15/02/2010].

[9] U.S. Environmental Protection Agency (EPA) - Testing and Measuring Emissions, Engine Brake Dynamometer Duty Cycles; 2009. See also: <www.epa.gov/nvfel/testing/dynamometer.htm#engcycles> [accessed 15/02/2010].

[10] Kang H, Farell PV. Experimental investigation of transient emissions (HC and NO_x) in a high speed direct injection (HSDI) diesel engine. SAE paper no. 2005-01-3883, 2005.

[11] Black J, Eastwood PG, Tufail K, Winstanley T, Hardalupas Y, Taylor AMKP. Diesel engine transient control and emissions response during a European extra-urban drive cycle (EUDC). SAE paper no. 2007-01-1938, 2007.

[12] Campbell B, Peckham M, Symonds J, Parkinson J, Finch A. Transient gaseous and particulate emissions measurements on a diesel passenger car including a DPF regeneration event. SAE paper no. 2006-01-1079, 2006.

[13] Rakopoulos CD, Dimaratos AM, Giakoumis EG, Peckham MS. Experimental assessment of turbocharged diesel engine transient emissions during acceleration, load change and starting. SAE paper no. 2010-01-1287, 2010.

[14] Hansen AC, Kyritsis DC, Lee CF. Characteristics of biofuels and renewable fuel standards. In: "Biomass to biofuels - Strategies for global industries", Vertes AA, Blaschek HP, Yukawa H, Qureshi N (editors). New York: John Wiley; 2009.

[15] Starr ME. Influence on transient emissions at various injection timings, using cetane improvers, bio-diesel, and low aromatic fuels. SAE paper no. 972904, 1997.

[16] Graboski MS, Ross JD, McCormick RL. Transient emissions from No. 2 diesel and biodiesel blends in a DDC Series 60 engine. SAE paper no. 961166, 1996.

[17] Sharp CA, Howell SA, Jobe J. The effect of biodiesel fuels on transient emissions from modern diesel engines - Part I: Regulated emissions and performance. SAE paper no. 2000-01-1967, 2000.

[18] Tsolakis A, Megaritis A, Wyszynski ML, Theinnoi K. Engine performance and emissions of a diesel engine operating on diesel-RME (rapeseed methyl ester) blends with EGR (exhaust gas recirculation). Energy 2007;32:2072-80.

[19] Wang WG, Lyons DW, Clark NN, Gautam M, Norton PM. Emissions from nine heavy trucks fueled by diesel and biodiesel blend without engine modification. Environ Sci Technol 2000;34:933-9.

[20] Durbin TD, Cocker DR III, Sawant AA, Johnson K, Miller JW, Holden BB, Helgeson NL, Jack JA. Regulated emissions from biodiesel fuels from on/off road applications. Atmos Environ 2007;41:5647-58.

[21] Karavalakis G, Tzirakis E, Zannikos F, Stournas S, Bakeas E, Arapaki N, Spanos A. Diesel/Soy methyl ester blends emissions profile from a passenger vehicle operated on the European and the Athens driving cycles. SAE paper no. 2007-01-4043, 2007.

[22] Luján JM, Bermúdez V, Tormos B, Pla B. Comparative analysis of a DI diesel engine fuelled with biodiesel blends during the European MVEG-A cycle: Performance and emissions (II). Biomass Bioenergy 2009;33:948-56.

[23] Fontaras G, Karavalakis G, Kousoulidou M, Tzamkiozis T, Ntziachristos L, Bakeas E, Stournas S, Samaras Z. Effects of biodiesel on passenger car fuel consumption, regulated and non-regulated pollutant emissions over legislated and real-world driving cycles. Fuel 2009;88:1608-17.

[24] Tsolakis A, Megaritis A, Yap D. Application of exhaust gas fuel reforming in diesel and homogeneous charge compression ignition (HCCI) engines fuelled with biofuels. Energy 2008;33:462-70.

[25] Ferreira SL, dos Santos AM, de Souza GR, Polito WL. Analysis of the emissions of volatile organic compounds from the compression ignition engine fueled by diesel-biodiesel blend and diesel oil using gas chromatography. Energy 2008;33:1801-6.

[26] Miers SA, Carlson RW, McConnell SS, Ng HK, Wallner T, Esper JL. Drive cycle analysis of butanol/diesel blends in a light-duty vehicle. SAE paper no. 2008-01-2381, 2008.

[27] Yoshimoto Y, Onodera M, Tamaki H. Performance and emission characteristics of diesel engines fueled by vegetable oils. SAE paper no. 2001-01-1807, 2001.

[28] Yoshimoto Y, Onodera M. Performance of a diesel engine fueled by rapeseed oil blended with oxygenated organic compounds. SAE paper no. 2002-01-2854, 2002.

[29] Huang J, Wang Y, Li S, Roskilly AP, Yu H, Li H. Experimental investigation on the performance and emissions of a diesel engine fuelled with ethanol-diesel blends. Appl Thermal Eng 2009;29:2484-90.

[30] Rakopoulos DC, Rakopoulos CD, Giakoumis EG, Dimaratos AM, Kyritsis DC. Effects of butanol-diesel fuel blends on the performance and emissions of a high-speed DI diesel engine. Energy Convers Manage 2010;51:1989-97.

[31] Armas O, Hernandez JJ, Cardenas MD. Reduction of diesel smoke opacity from vegetable oil methyl ester during transient operation. Fuel 2006;85:2427-38.

[32] Armas O, Cardenas MD, Mata C. Smoke opacity and NO_x emissions from a bioethanol-diesel blend during engine transient operation. SAE paper no. 2007-24-0131, 2007.

[33] CLD500 NO_x analyzer, Cambustion Ltd., Cambridge, UK. See also: <www.cambustion.co.uk> [accessed 10/02/2010].

[34] CLD500 Fast NO_x Measurement System, User Manual (version 2.2), Cambustion Ltd., 2008.

[35] AVL 439 Opacimeter, Operating Manual, AVL, November 2006.

[36] Papayannakos N, Rakopoulos CD, Kyritsis S, Lappas A, Chatzigakis A, Chlivinos G, Liakopoulos I, Siragakis G. Pilot production and testing of bio-diesel produced from Greek feedstocks. In: C. Frangopoulos, C. Rakopoulos, G. Tsatsaronis, editors. Proc. of 19th Int. Conference 'ECOS 2006', Crete, Greece, July 12-14, 2006, vol. 3, p. 1489-97.

[37] Rakopoulos CD, Antonopoulos KA, Rakopoulos DC. Experimental heat release analysis and emissions of a HSDI diesel engine fueled with ethanol-diesel fuel blends. Energy 2007;32:1791-808.

[38] DieselNet, Ecopoint Inc., Technical Data Sheets, Smoke Opacity Paper. See also: <www.dieselnet.com/calculator/smoke1.html> [accessed 30/01/2010].

[39] Lakshmanan T, Nagarajan G. Experimental investigation of timed manifold injection of acetylene in direct injection diesel engine in dual fuel mode. Energy 2010;35:3172-8.

[40] Andrews GE, Clarke AG, Rojas NY, Sale T, Gregory D. The transient storage and blow-out of diesel particulate in practical exhaust systems. SAE paper no. 2001-01-0204, 2001.

[41] Rakopoulos CD, Antonopoulos KA, Rakopoulos DC. Multi-zone modeling of diesel engine fuel spray development with vegetable oil, bio-diesel or diesel fuels. Energy Convers Manage 2006;47:1550-73.

Figures Captions

Fig. 1   Schematic arrangement of the test bed installation, instrumentation and data acquisition system

Fig. 2   Initial and final conditions of each transient test examined

Fig. 3   Qualitative fuel pump rack and boost pressure response (lower subfigure), and NO concentration and smoke opacity development (upper subfigure) during a typical acceleration case

Fig. 4   Development of engine and turbocharger parameters and emissions response during the acceleration Test No. 1

Fig. 5   Expanded view of smoke emissions during the acceleration Test No. 1

Fig. 6   Maximum values of the global gas temperature and of the exhaust NO emission values at each cycle of the acceleration Test No. 1

Fig. 7   Cumulative NO and soot mass during the acceleration Test No. 1

Fig. 8   Development of engine and turbocharger parameters and emissions response during the acceleration Test No. 2

Fig. 9   Expanded view of smoke emissions during the acceleration Test No. 2

Fig. 10   Cumulative NO and soot mass during the acceleration Test No. 2

Fig. 11   Development of engine and turbocharger parameters and emissions response during the acceleration Test No. 3

Fig. 12   Cumulative NO and soot mass during the acceleration Test No. 3

Tables Captions

Table 1   Engine and turbocharger specifications

Table 2   Measuring devices for the engine and turbocharger operating parameters and their measuring error

Table 3   Properties of diesel fuel, methyl esters (ME) of sunflower and cottonseed oils, and n-butanol (normal butanol)

Table 4   Tabulation of test conditions examined

Table 5   Percentage changes of peak pollutant emissions values for the two fuel blends examined, compared to the baseline (100% diesel fuel)

Table 1

Engine model and type	'Mercedes Benz', OM 366 LA, 6 cylinder, in-line, 4-stroke, compression ignition, direct injection, water-cooled, turbocharged, after-cooled, with bowl-in-piston
Emissions standard	Euro II
Speed range	800–2600 rpm
Maximum power	177 kW @ 2600 rpm
Maximum torque	840 Nm @ 1250–1500 rpm
Engine total displacement	5958 cm^3
Bore/Stroke	97.5mm/133 mm
Compression ratio	18:1
Fuel pump	'Bosch' PE-S series, in-line, 6-cylinder with fuel limiter
Static injection timing	5±1° crank angle before TDC (at full load)
Turbocharger model	'Garrett' TBP 418-1 with internal waste-gate
Aftercooler	Air-to-Air

Table 2

Parameter	Measuring device	Error
Engine speed	'Kistler' shaft encoder	0.02° CA
Cylinder pressure	'Kistler' miniature piezoelectric transducer, combined with 'Kistler' charge amplifier	< ±1% FSO
Fuel pump rack position	Linear Variable Differential Transducer (LVDT)	0.1 mm
Boost pressure	'Wika' pressure transmitter	< ±1% FSO
Turbocharger speed	'Garrett' turbo speed sensor (including gauge)	± 0.5% FSO

Table 3

Fuel properties	Diesel fuel	Sunflower ME	Cottonseed ME	N-Butanol
Density at 20ºC, kg/m^3	837	880	885	810
Cetane number	50	50	52	~25
Lower calorific value, MJ/kg	43	37.5	37.5	33.1
Kinematic viscosity at 40ºC, mm^2/s	2.6	4.4	4	3.6[+]
Boiling point	180-360	345	345	118
Latent heat of evaporation, kJ/kg	250	230	230	585
Oxygen, % weight	0	10.9	10.9	21.6
Stoichiometric air-fuel ratio	15.0	12.5	12.5	11.2
Molecular weight	170	284	284	74

[+]Measured at 20ºC

Table 4

Test No.	Initial Conditions		Final Conditions	
	Speed (rpm)	Load (%)	Speed (rpm)	Load (%)
1.	1016	10	1880	15
2.	1530	10	2080	20
3.	1530	40	2055	75

Table 5

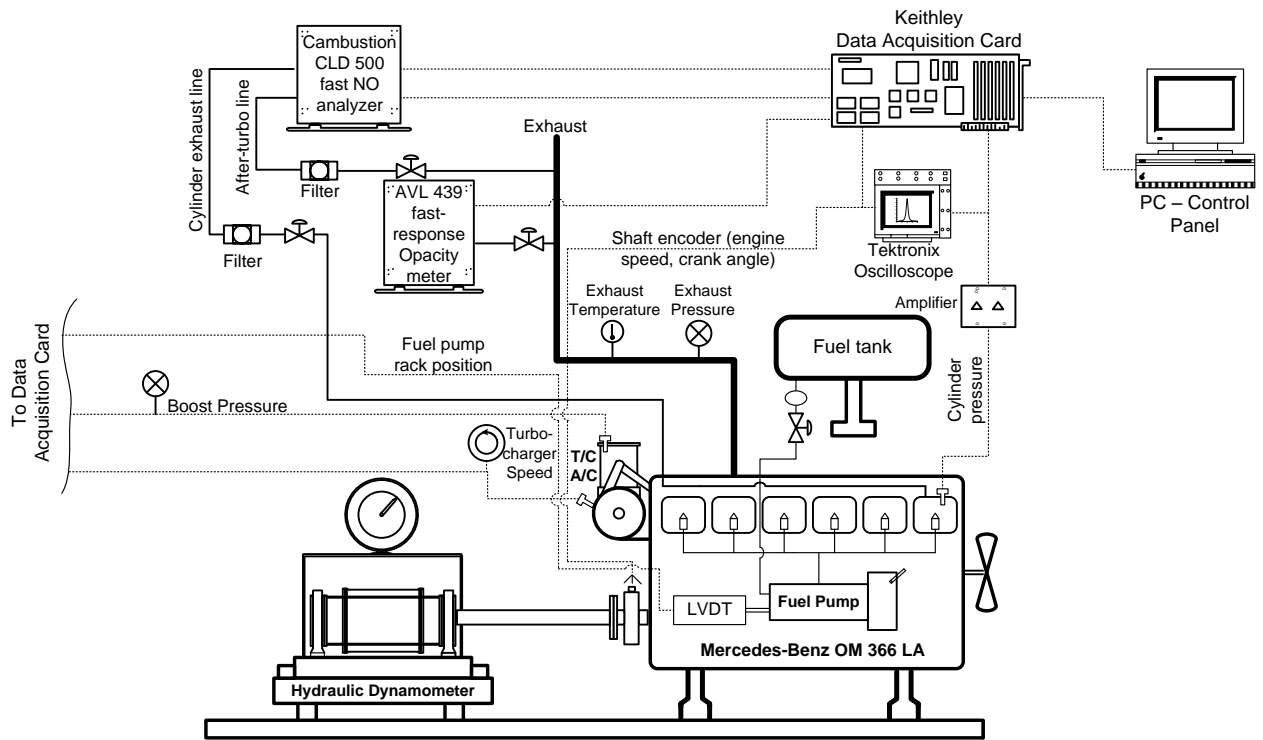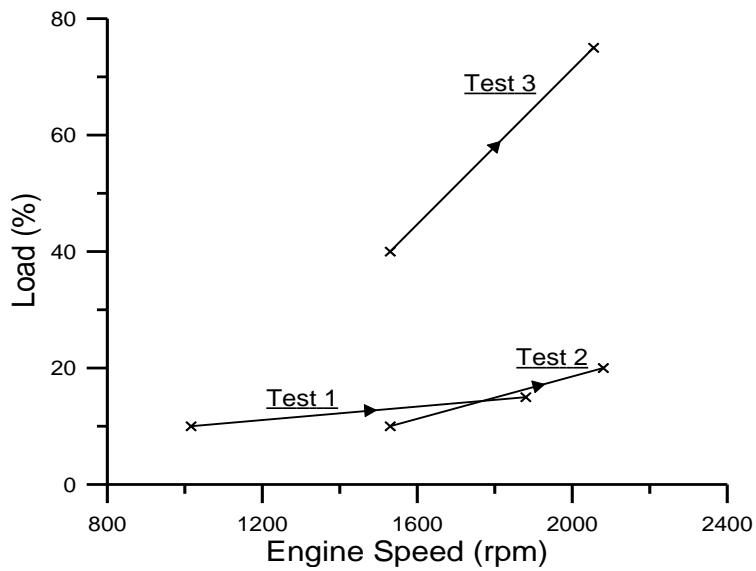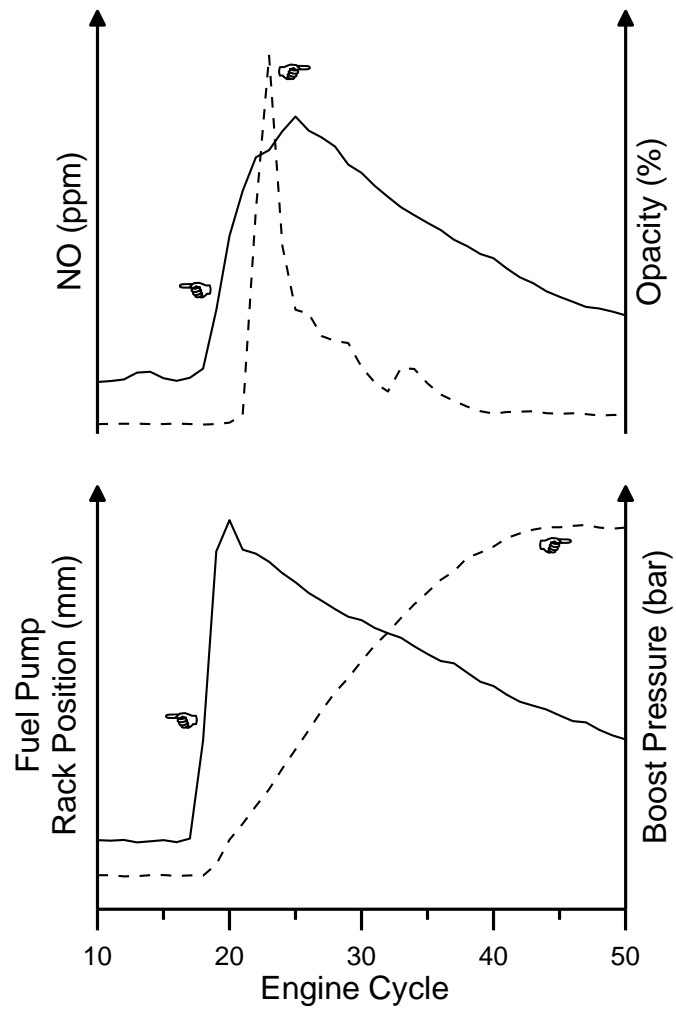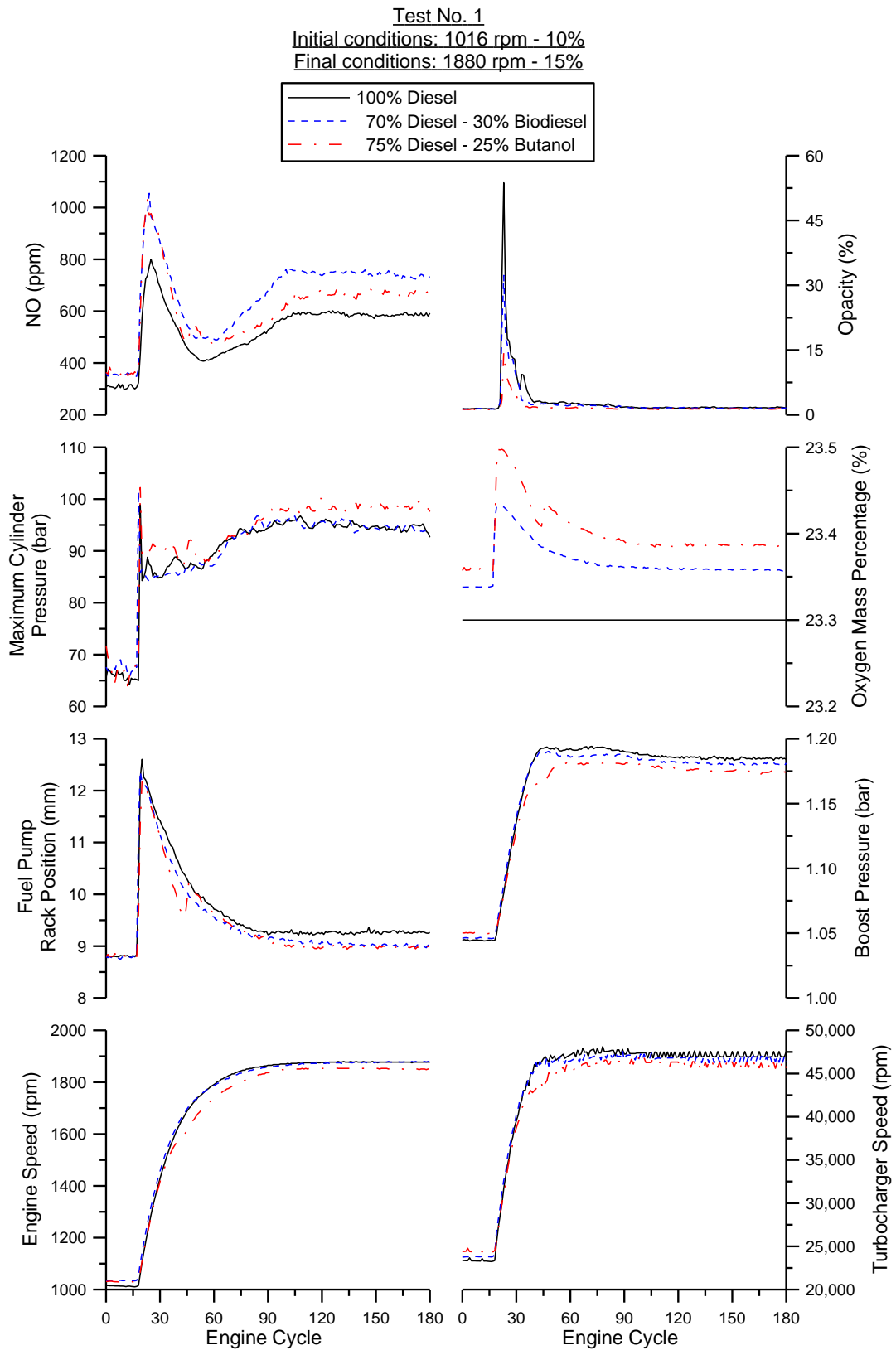| Fuel blend	Test No. 1		Test No. 2		Test No. 3	
	NO (%)	Soot (%)	NO (%)	Soot (%)	NO (%)	Soot (%)
70% Diesel - 30% Bio-diesel	31.7	-39.9	44.4	-13.3	51.5	-30.1
75% Diesel - 25% N-Butanol	28.7	-72.9	33.8	-50.4	34.6	-55.5

Fig. 1. Rakopoulos et al.

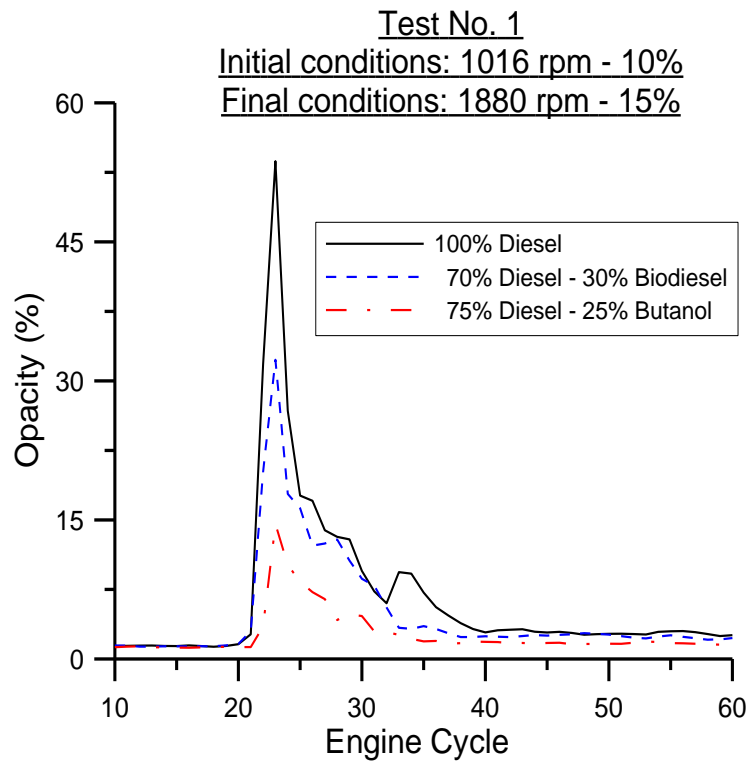

Fig. 2. Rakopoulos et al.

Fig. 3. Rakopoulos et al.

Test No. 1
Initial conditions: 1016 rpm - 10%
Final conditions: 1880 rpm - 15%

——— 100% Diesel
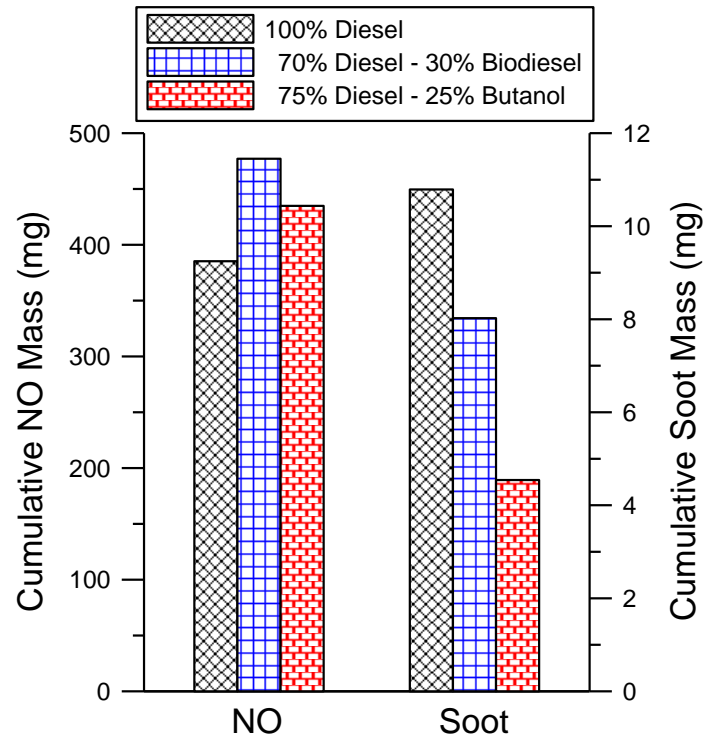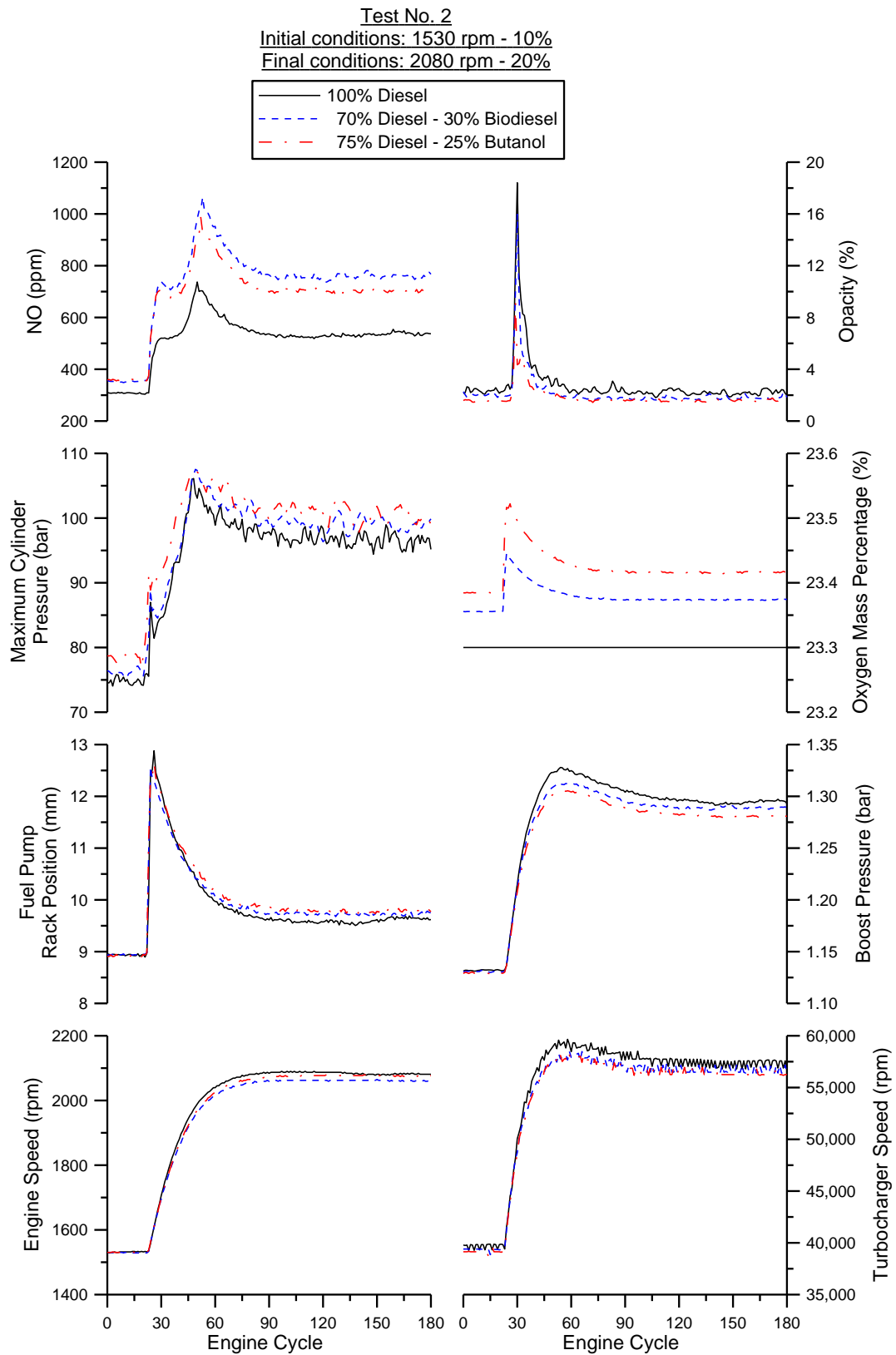- - - - 70% Diesel - 30% Biodiesel
—·—·— 75% Diesel - 25% Butanol

Fig. 4. Rakopoulos et al.

28

Fig. 5. Rakopoulos et al.
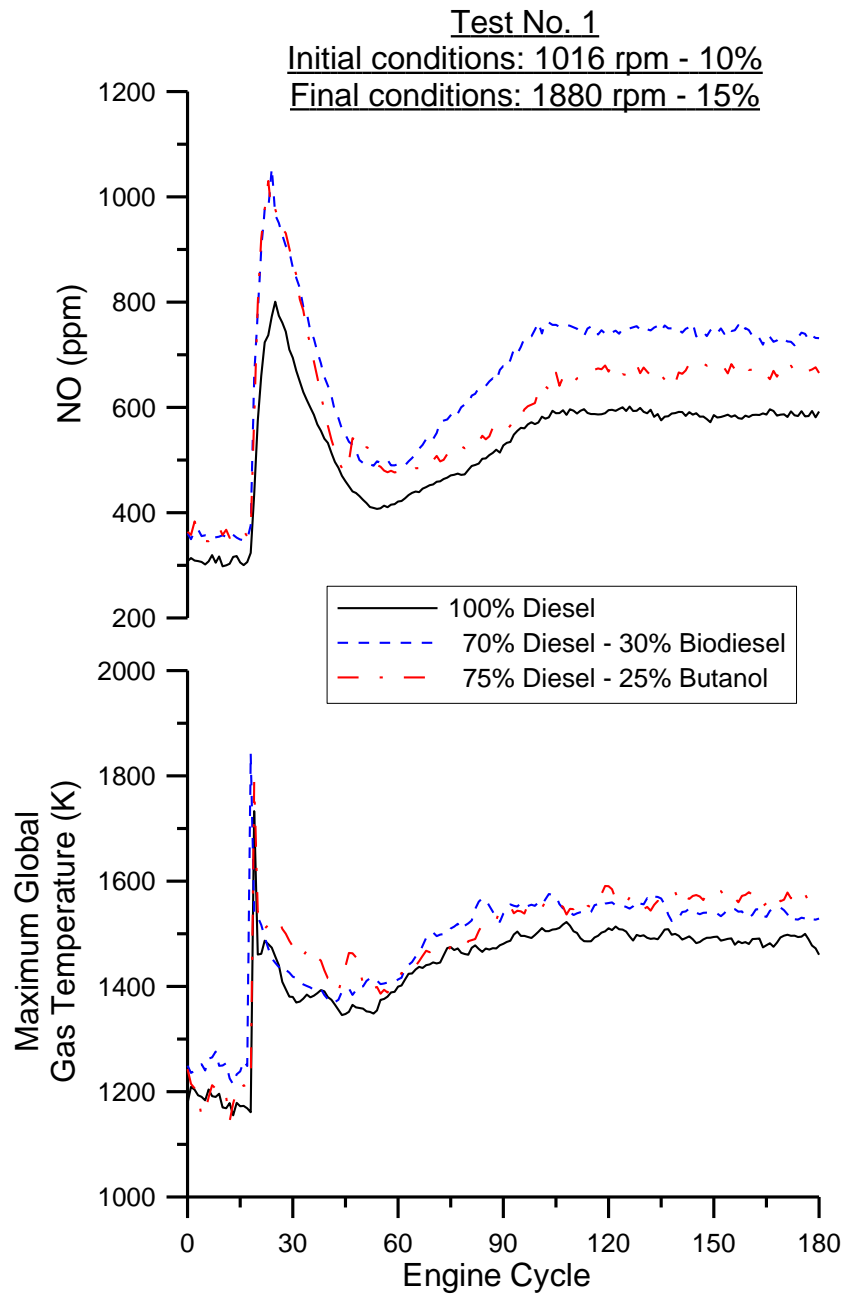
Test No. 1
Initial conditions: 1016 rpm - 10%
Final conditions: 1880 rpm - 15%

Legend:
— 100% Diesel
- - - 70% Diesel - 30% Biodiesel
- · — 75% Diesel - 25% Butanol

Fig. 6. Rakopoulos et al.

Fig. 7. Rakopoulos et al.

Test No. 2
Initial conditions: 1530 rpm - 10%
Final conditions: 2080 rpm - 20%

100% Diesel
70% Diesel - 30% Biodiesel
75% Diesel - 25% Butanol

Fig. 8. Rakopoulos et al.

Fig. 9. Rakopoulos et al.

Test No. 2
Initial conditions: 1530 rpm - 10%
Final conditions: 2080 rpm - 20%
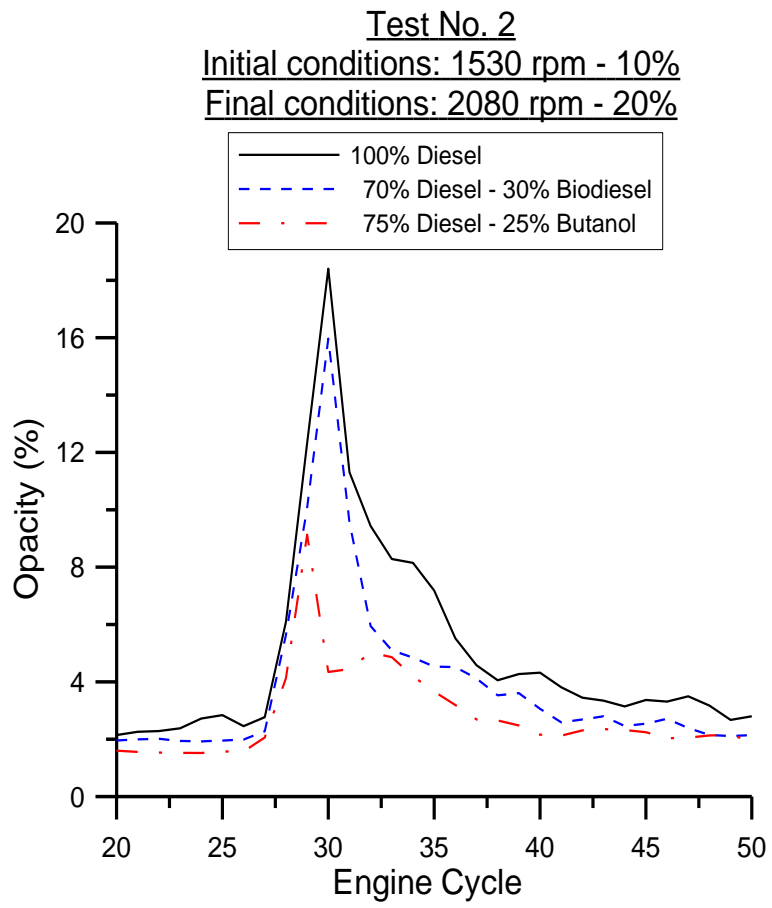
Legend:
- 100% Diesel
- 70% Diesel - 30% Biodiesel
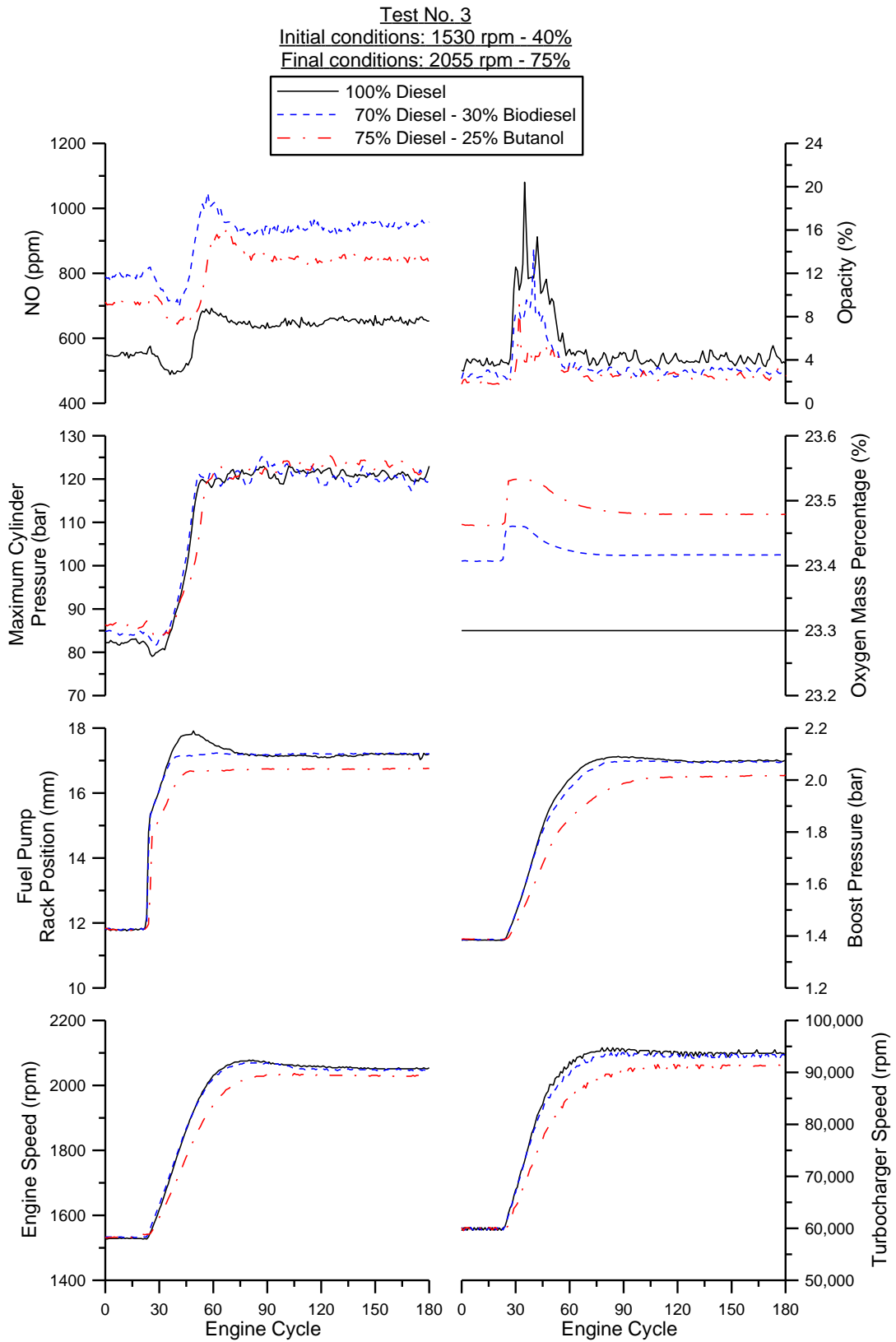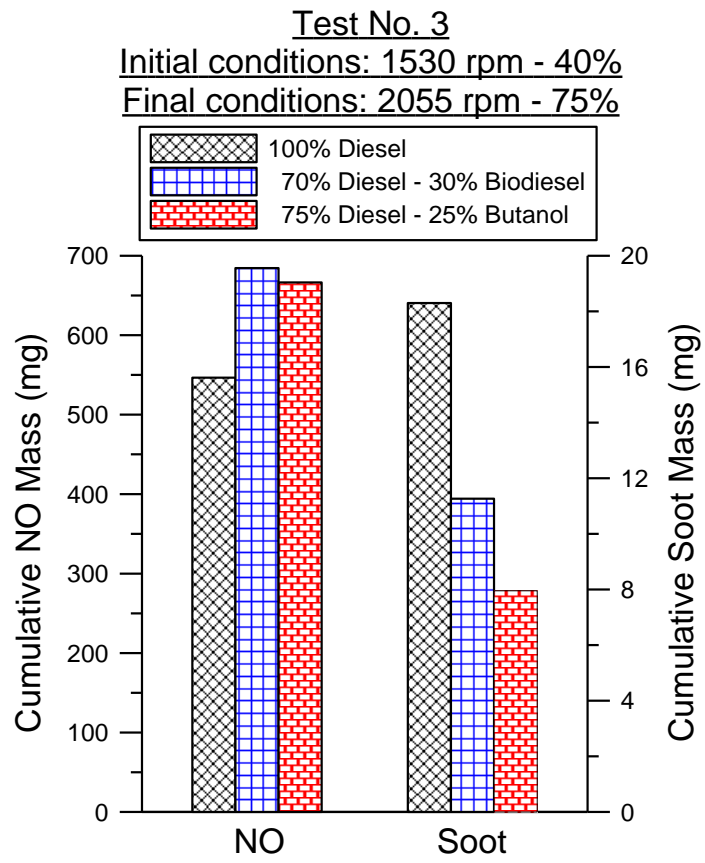- 75% Diesel - 25% Butanol
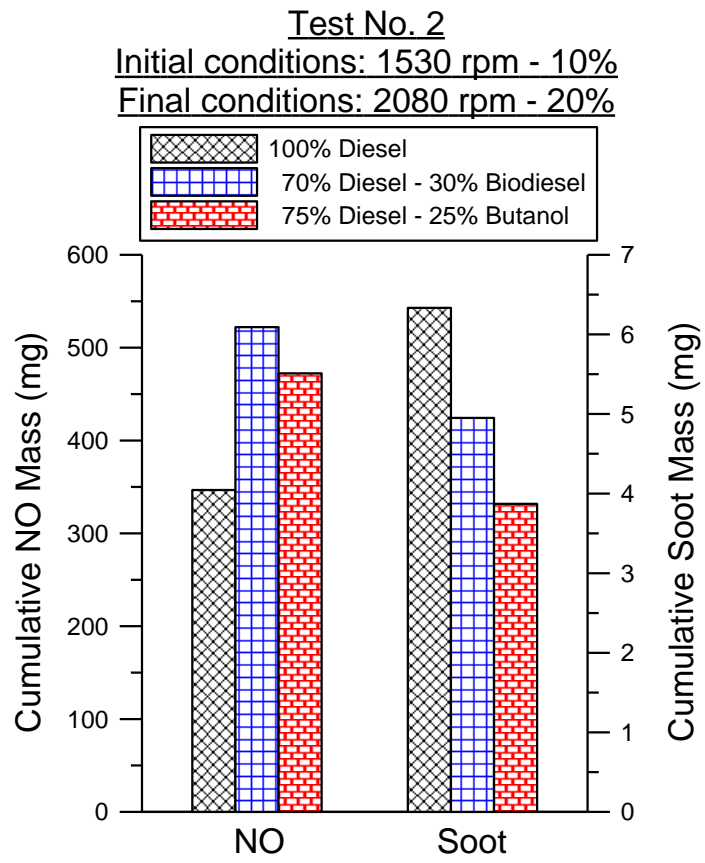
Fig. 10. Rakopoulos et al.

Fig. 11. Rakopoulos et al.

Fig. 12. Rakopoulos et al.